Broken symmetries and lattice gauge theory (I): LGT, a theoretical femtoscope for non-perturbative strong dynamics

Leonardo Giusti

University of Milano-Bicocca

Quantum Chromodynamics (QCD)

- QCD is the quantum field theory of strong interactions in Nature. Its action

[Fritzsch, Gell-Mann, Leutwyler 73; Gross, Wilczek 73; Weinberg 73]

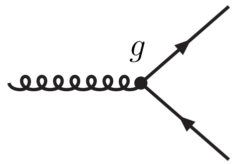

$$S[A, \bar{\psi}_i, \psi_i; g, m_i, \theta]$$

is fixed by few simple principles:

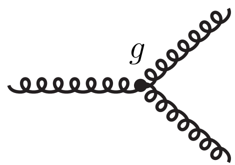

∗ SU(3)$_c$ gauge (local) invariance

∗ Quarks in fundamental representation $\psi_i = u, d, s, c, b, t$

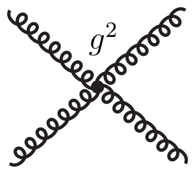

∗ Renormalizability

- Present experimental results compatible with $\theta = 0$

- It is fascinating that such a simple action and few parameters $[g, m_i]$ can account for the variety and richness of strong-interaction physics phenomena

Asymptotic freedom

- The renormalized coupling constant is scale dependent

$$\mu \frac{d}{d\mu} g = \beta(g)$$

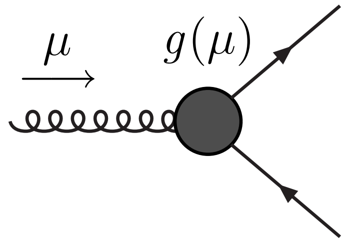

and QCD is asymptotically free [$b_0 > 0$]
[Gross, Wilczek 73; Politzer 73]

$$\beta(g) = -b_0 g^3 - b_1 g^5 + \ldots$$

- The theory develops a fundamental scale

$$\Lambda = \mu \left[b_0 g^2(\mu)\right]^{-b_1/2b_0^2} e^{-\frac{1}{2b_0 g^2(\mu)}} e^{-\int_0^{g(\mu)} dg \left[\frac{1}{\beta(g)} + \frac{1}{b_0 g^3} - \frac{b_1}{b_0^2 g}\right]}$$

which is a non-analytic function of the coupling constant at $g^2 = 0$. Quantization breaks scale invariance at $m_i = 0$

Perturbative corner: hard processes

[PDG 2014]

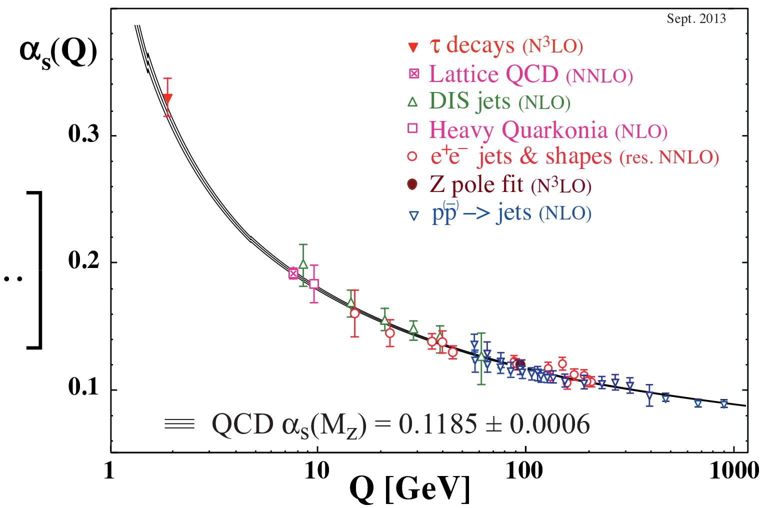

- Processes where the relevant energy scale is $\mu \gg \Lambda$ can be studied by pert. expansion

$$\alpha_s(\mu) = \frac{g^2(\mu)}{4\pi} = \frac{1}{4\pi b_0 \ln\left(\frac{\mu^2}{\Lambda^2}\right)}\left[1 - \frac{b_1}{b_0^2}\frac{\ln(\ln(\frac{\mu^2}{\Lambda^2}))}{\ln(\frac{\mu^2}{\Lambda^2})} + \ldots\right]$$

- An example is given by

$$R = \frac{\sigma(e^+e^- \to \text{hadrons})}{\sigma(e^+e^- \to \mu^+\mu^-)}$$

$$= 3\sum_i Q_i^2 \cdot \left[1 + \frac{\alpha_s(\mu)}{\pi} + C_2\left(\frac{\alpha_s(\mu)}{\pi}\right)^2 + \cdots\right]$$

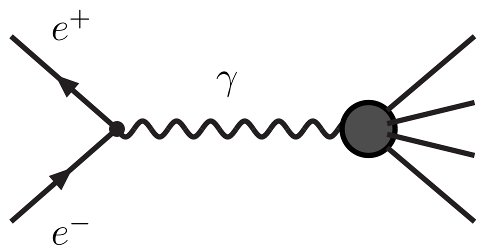

- Experimental results significantly prove the logarithmic dependence in μ/Λ predicted by perturbative QCD

Scale of the strong interactions

- By comparing these measurements to theory

$$\Lambda \sim 0.2 \text{ GeV} \qquad 1/\Lambda \sim 1 \text{ fm} = 10^{-15} \text{ m}$$

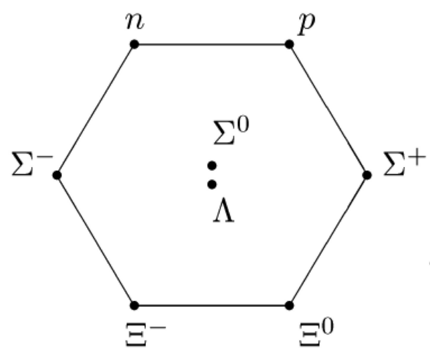

- At these distances the dynamics of QCD is non-perturbative

- A rich spectrum of hadrons is observed at these energies. Their properties such as

$$M_n = b_n \, \Lambda$$

need to be computed non-perturbatively

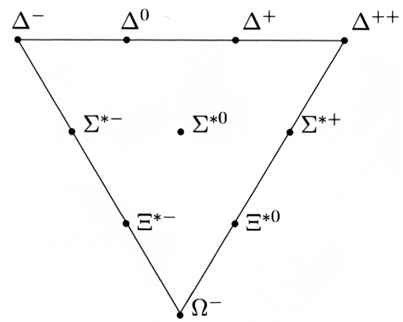

- The theory is highly predictive: in the (interesting) limit $m_{u,d,s} = 0$ and $m_{c,b,t} \to \infty$, for instance, dimensionless quantities are parameter-free numbers

- Octet compatible with SSB pattern

$$\text{SU}(3)_\text{L} \times \text{SU}(3)_\text{R} \to \text{SU}(3)_\text{L+R}$$

and soft explicit symmetry breaking

$$m_u, m_d \ll m_s < \Lambda$$

- $m_u, m_d \ll m_s \Longrightarrow m_\pi \ll m_\text{K}$

- A 9^th pseudoscalar with $m_{\eta'} \sim \mathcal{O}(\Lambda)$

I	I_3	S	Meson	Quark Content	Mass (GeV)
1	1	0	π^+	$u\bar{d}$	0.140
1	-1	0	π^-	$d\bar{u}$	0.140
1	0	0	π^0	$(d\bar{d} - u\bar{u})/\sqrt{2}$	0.135
$\frac{1}{2}$	$\frac{1}{2}$	+1	K^+	$u\bar{s}$	0.494
$\frac{1}{2}$	-$\frac{1}{2}$	+1	K^0	$d\bar{s}$	0.498
$\frac{1}{2}$	-$\frac{1}{2}$	-1	K^-	$s\bar{u}$	0.494
$\frac{1}{2}$	$\frac{1}{2}$	-1	$\overline{\text{K}}^0$	$s\bar{d}$	0.498
0	0	0	η	$\cos\vartheta\eta_8 - \sin\vartheta\eta_0$	0.548
0	0	0	η'	$\sin\vartheta\eta_8 + \cos\vartheta\eta_0$	0.958

$$\eta_8 = (d\bar{d} + u\bar{u} - 2s\bar{s})/\sqrt{6}$$
$$\eta_0 = (d\bar{d} + u\bar{u} + s\bar{s})/\sqrt{3}$$
$$\vartheta \sim -10^\circ$$

- QCD action for $N_F = 2$, $M^\dagger = M = \text{diag}(m, m)$

$$S = S_G + \int d^4x \left\{ \bar\psi D \psi + \bar\psi_{\rm R} M^\dagger \psi_{\rm L} + \bar\psi_{\rm L} M \psi_{\rm R} \right\} , \qquad D = \gamma_\mu(\partial_\mu - i A_\mu)$$

- For $M = 0$ chiral symmetry

$$\psi_{\rm R,L} \rightarrow V_{\rm R,L} \psi_{\rm R,L} \qquad \psi_{\rm R,L} = \left(\frac{1 \pm \gamma_5}{2}\right) \psi$$

Chiral anomaly: measure not invariant

SSB: vacuum not symmetric

$${\rm SU}(3)_c \times {\rm SU}(2)_{\rm L} \times {\rm SU}(2)_{\rm R} \times {\rm U}(1)_{\rm L} \times {\rm U}(1)_{\rm R} \times \mathcal{R}_{\rm scale}$$

$\downarrow$ **(dim. transm., chiral anomaly)**

$${\rm SU}(3)_c \times {\rm SU}(2)_{\rm L} \times {\rm SU}(2)_{\rm R} \times {\rm U}(1)_{\rm B=L+R}$$

$\downarrow$ **(Spont. Sym. Break.)**

$${\rm SU}(3)_c \times {\rm SU}(2)_{\rm L+R} \times {\rm U}(1)_{\rm B}$$

$\downarrow$ (Confinement)

$${\rm SU}(2)_{\rm L+R} \times {\rm U}(1)_{\rm B}$$

- Breaking due to non-perturbative dynamics. Precise quantitative tests are being made on the lattice

Lattice QCD: action [Wilson 74]

- QCD can be defined on a discretized space-time so that gauge invariance is preserved
- Quark fields reside on four-dimensional lattice, the gauge field $U_\mu \in \mathrm{SU}(3)$ resides on links

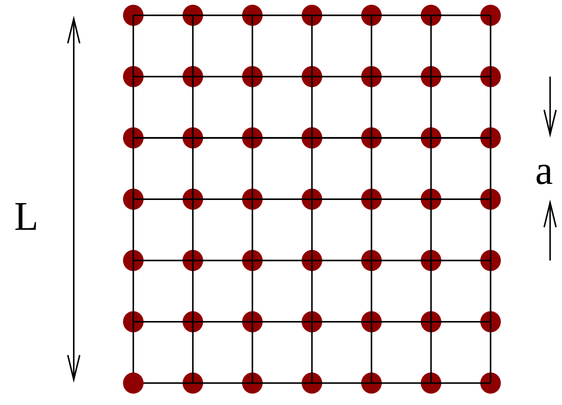

- The Wilson action for the gauge field is

$$S_G[U] = \frac{\beta}{2} \sum_x \sum_{\mu,\nu} \left[1 - \frac{1}{3} \mathrm{ReTr} \left\{ U_{\mu\nu}(x) \right\} \right]$$

where $\beta = 6/g^2$ and the plaquette is

$$U_{\mu\nu}(x) = U_\mu(x)\, U_\nu(x+\hat{\mu})\, U_\mu^\dagger(x+\hat{\nu})\, U_\nu^\dagger(x)$$

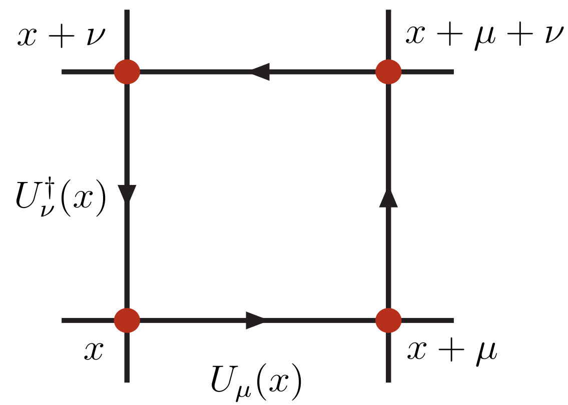

- Popular discretizations of fermion action: Wilson, Domain-Wall-Neuberger, tmQCD

Lattice QCD: path integral [Wilson 74]

- The lattice provides a non-perturbative definition of QCD. The path integral at finite spacing and volume is mathematically well defined (Euclidean time)

$$Z = \int DU D\bar{\psi}_i D\psi_i \; e^{-S[U,\bar{\psi}_i,\psi_i;g,m_i]}$$

- Nucleon mass, for instance, can be extracted from the behaviour of a suitable two-point correlation function at large time-distance

$$\langle O_N(x)\bar{O}_N(y)\rangle = \frac{1}{Z}\int DU D\bar{\psi}_i D\psi_i \; e^{-S}\, O_N(x)\bar{O}_N(y) \longrightarrow R_N\; e^{-M_N\,|x_0-y_0|}$$

- For small gauge fields, the pert. expansion differs from usual one for terms of $O(a)$

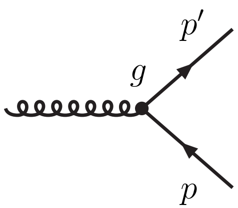

$$= -igT^a\left\{\gamma_\mu - \tfrac{i}{2}(p_\mu + p'_\mu)a + O(a^2)\right\}$$

Consistency of lattice QCD with standard perturbative approach is thus guaranteed

Lattice QCD: universality

- Continuum and infinite-volume limit of Lattice QCD is the $non\text{-}perturbative$ $definition$ of QCD

- Details of the discretization become irrelevant in the continuum limit, and any reasonable lattice formulation tends to the same continuum theory

$$M_N(a) = M_N + c_N a + \ldots$$

Lattice QCD: universality

- Continuum and infinite-volume limit of Lattice QCD is the *non-perturbative definition* of QCD

- Details of the discretization become irrelevant in the continuum limit, and any reasonable lattice formulation tends to the same continuum theory

$$M_N(a) = M_N + d_N a^2 + \dots$$

- By a proper tuning of the action and operators, convergence to continuum can be accelerated without introducing extra free-parameters
[Symanzik 83; Sheikholeslami Wohlert 85; Lüscher et al. 96]

- Finite-volume effects are proportional to $\exp(-M_\pi L)$ at asymptotically large volumes

Numerical lattice QCD: machines

- Correlation functions at $finite\ volume$ and $finite\ lattice\ spacing$ can be computed by Monte Carlo techniques $exactly$ up to statistical errors

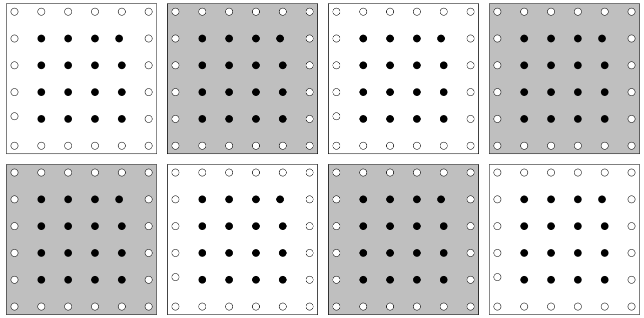

[Galileo – CINECA]

- Look at quantities not accessible to experiments:

  $*$ quark mass dependence

  $*$ volume dependence

  $*$ unphysical quantities $\Sigma, \chi, \ldots$

  for understanding...

Numerical lattice QCD: machines

- Typical lattice parameters:

$a \ = 0.05$ fm $\qquad (a\Lambda)^2 \sim 0.25\%$

$L = 3.2$ fm $\qquad \Longrightarrow \qquad M_\pi L \geq 4, \quad M_\pi \geq 0.25$ GeV

$V = 2L \times L^3 \qquad$ #points $= 2^{25} \sim 3.4 \cdot 10^7$

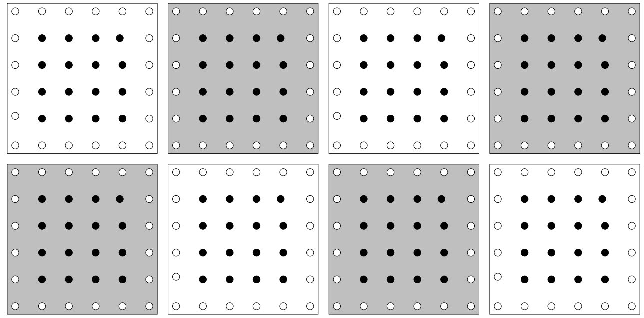

- Monte Carlo algorithms integrate over 10^7–10^9 SU(3) link variables

- A typical cluster of PCs:

  $*$ Standard CPUs [Intel, AMD]

  $*$ Fast connection [40Gbit/s]

[Galileo – CINECA]

- Lattice partitioned in blocks which are distributed over the nodes (256×16 a good example)

- Data exchange among nodes minimized thanks to the locality of the action

Numerical lattice QCD: algorithms

- Extraordinary algorithmic progress over the last 30 years, keywords:
  - $*$ Hybrid Monte Carlo (HMC)
    Duane et al. 87
  - $*$ Multiple time-step integration
    Sexton, Weingarten 92
  - $*$ Frequency splitting of determinant
    Hasenbusch 01
  - $*$ Domain Decomposition
    Lüscher 04
  - $*$ Mass preconditioning and rational HMC
    Urbach et al 05; Clark, Kennedy 06
  - $*$ Deflation of low quark modes
    Lüscher 07
  - $*$ Avoiding topology freezing
    Lüscher, Schaefer 12

[Della Morte et al. 05]

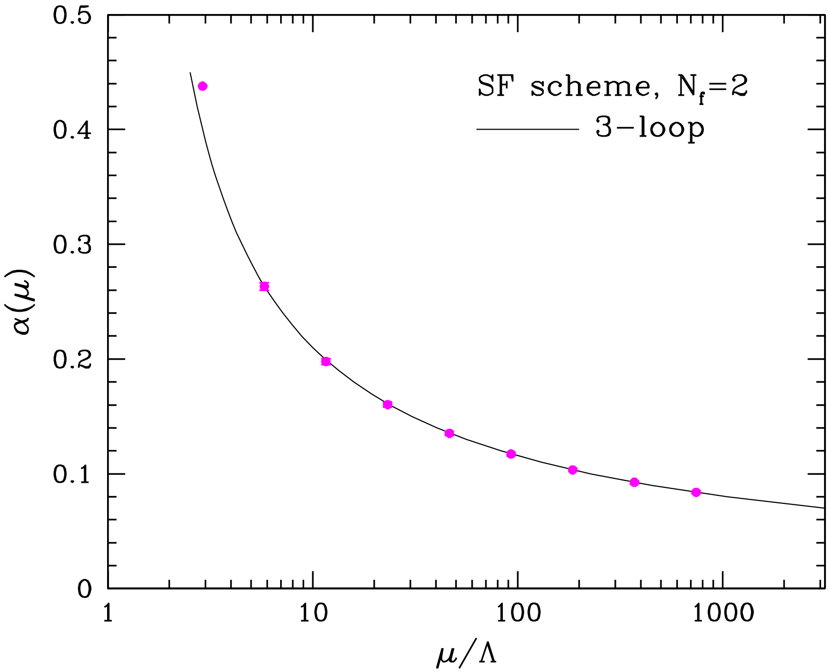

- Light dynamical quarks can be simulated. Chiral regime of QCD is accessible
- Algorithms are designed to produce exact results up to statistical errors

Numerical lattice QCD: algorithms

- Extraordinary algorithmic progress over the last 30 years, keywords:

  ∗ Hybrid Monte Carlo (HMC)
  Duane et al. 87

  ∗ Multiple time-step integration
  Sexton, Weingarten 92

  ∗ Frequency splitting of determinant
  Hasenbusch 01

  ∗ Domain Decomposition
  Lüscher 04

  ∗ Mass preconditioning and rational HMC
  Urbach et al 05; Clark, Kennedy 06

  ∗ Deflation of low quark modes
  Lüscher 07

  ∗ Avoiding topology freezing
  Lüscher, Schaefer 12

[BMW Collaboration 09]

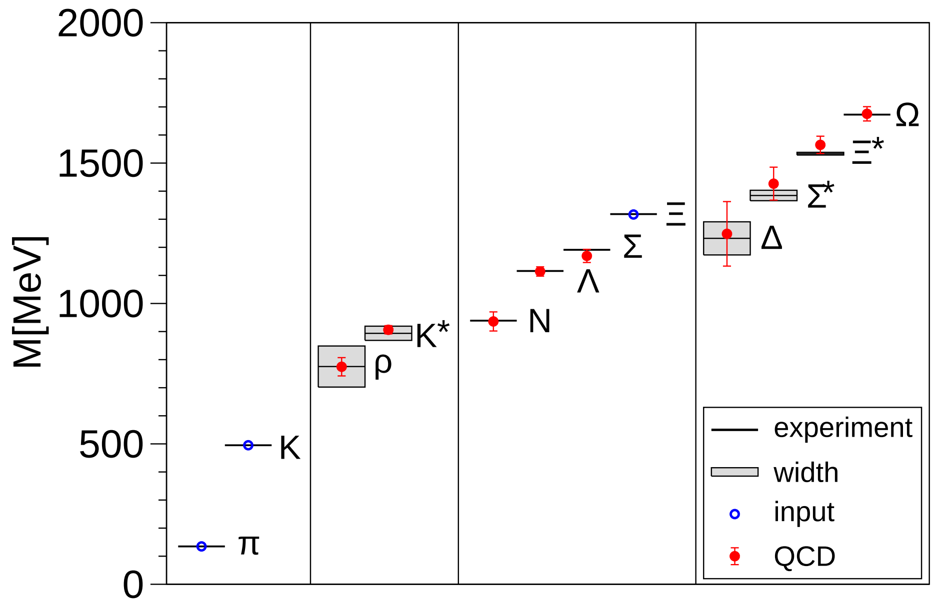

- Light dynamical quarks can be simulated. Chiral regime of QCD is accessible
- Algorithms are designed to produce exact results up to statistical errors

Lattice QCD: a theoretical femtoscope

- Lattice QCD is the femtoscope for studying strong dynamics. Its lenses are made of quantum field theory, numerical techniques and computers
- It allows us to look also at quantities not accessible to experiments which may help understanding the underlying mechanisms
- Femtoscope still rather crude. Often we compute what we can and not what would like to
- An example: the signal-to-noise ratio of the nucleon two-point correlation function

$$\frac{\langle O_N \bar{O}_N \rangle^2}{\Delta^2} \propto n\, e^{-(2M_N - 3M_\pi)|x_0 - y_0|}$$

decreases exp. with time-distance of sources.
At physical point $2M_N - 3M_\pi \simeq$ 7 fm^{-1}

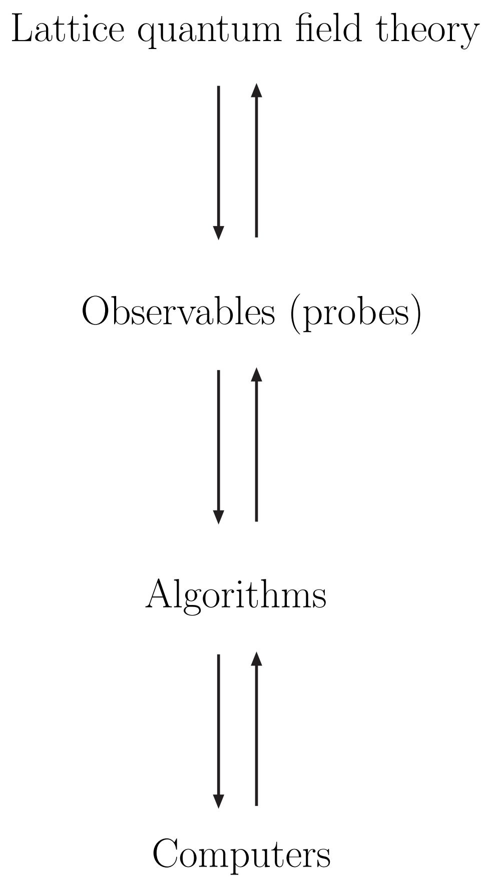

Lattice QCD: a theoretical femtoscope

- Lattice QCD is the femtoscope for studying strong dynamics. Its lenses are made of quantum field theory, numerical techniques and computers
- It allows us to look also at quantities not accessible to experiments which may help understanding the underlying mechanisms
- Femtoscope still rather crude. Often we compute what we can and not what would like to
- A rather general strategy is emerging: design special purpose algorithms which exploit known math. and phys. properties of the theory to be faster
- Results from first-principles when all syst. uncertainties quantified. This achieved without introducing extra free parameters or dynamical assumptions but just by improving the femtoscope

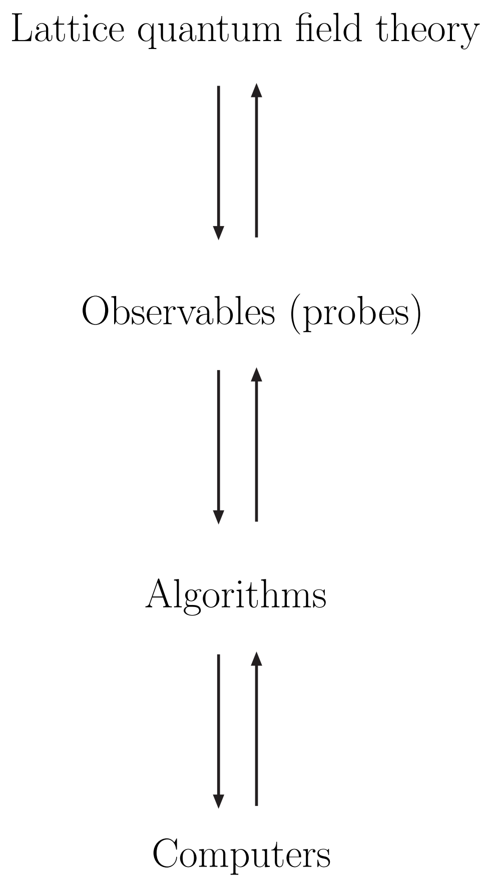

Broken symmetries and lattice gauge theory (II and III): chiral anomaly and the Witten–Veneziano mechanism

Leonardo Giusti

University of Milano-Bicocca

Light pseudoscalar meson spectrum

- Octet compatible with SSB pattern

$$\mathrm{SU}(3)_\mathrm{L} \times \mathrm{SU}(3)_\mathrm{R} \to \mathrm{SU}(3)_{\mathrm{L+R}}$$

and soft explicit symmetry breaking

$$m_u, m_d \ll m_s < \Lambda$$

- $m_u, m_d \ll m_s \Longrightarrow m_\pi \ll m_\mathrm{K}$

- A 9^{th} pseudoscalar with $m_{\eta'} \sim \mathcal{O}(\Lambda)$

I	I_3	S	Meson	Quark Content	Mass (GeV)
1	1	0	π^+	$u\bar{d}$	0.140
1	-1	0	π^-	$d\bar{u}$	0.140
1	0	0	π^0	$(d\bar{d} - u\bar{u})/\sqrt{2}$	0.135
$\frac{1}{2}$	$\frac{1}{2}$	+1	K^+	$u\bar{s}$	0.494
$\frac{1}{2}$	-$\frac{1}{2}$	+1	K^0	$d\bar{s}$	0.498
$\frac{1}{2}$	-$\frac{1}{2}$	-1	K^-	$s\bar{u}$	0.494
$\frac{1}{2}$	$\frac{1}{2}$	-1	$\overline{\mathrm{K}}^0$	$s\bar{d}$	0.498
0	0	0	η	$\cos\vartheta\eta_8 - \sin\vartheta\eta_0$	0.548
0	0	0	η'	$\sin\vartheta\eta_8 + \cos\vartheta\eta_0$	0.958

$$\eta_8 = (d\bar{d} + u\bar{u} - 2s\bar{s})/\sqrt{6}$$

$$\eta_0 = (d\bar{d} + u\bar{u} + s\bar{s})/\sqrt{3}$$

$$\vartheta \sim -10^\circ$$

QCD action and its (broken) symmetries

- QCD action for $N_F = 2$, $M^\dagger = M = \text{diag}(m, m)$

$$S = S_G + \int d^4x \left\{ \bar\psi D\psi + \bar\psi_{\rm R} M^\dagger \psi_{\rm L} + \bar\psi_{\rm L} M \psi_{\rm R} \right\}, \qquad D = \gamma_\mu(\partial_\mu - iA_\mu)$$

- For $M = 0$ chiral symmetry

$$\psi_{\rm R,L} \to V_{\rm R,L}\psi_{\rm R,L} \qquad \psi_{\rm R,L} = \left(\frac{1 \pm \gamma_5}{2}\right)\psi$$

Chiral anomaly: measure not invariant

SSB: vacuum not symmetric

$${\rm SU}(3)_c \times {\rm SU}(2)_{\rm L} \times {\rm SU}(2)_{\rm R} \times {\rm U}(1)_{\rm L} \times {\rm U}(1)_{\rm R} \times \mathcal{R}_{\rm scale}$$

↓ (dim. transm., chiral anomaly)

$${\rm SU}(3)_c \times {\rm SU}(2)_{\rm L} \times {\rm SU}(2)_{\rm R} \times {\rm U}(1)_{\rm B=L+R}$$

↓ (Spont. Sym. Break.)

$${\rm SU}(3)_c \times {\rm SU}(2)_{\rm L+R} \times {\rm U}(1)_{\rm B}$$

↓ (Confinement)

$${\rm SU}(2)_{\rm L+R} \times {\rm U}(1)_{\rm B}$$

- Breaking due to non-perturbative dynamics. Precise quantitative tests are being made on the lattice

Numerical challenge

- A Monte Carlo computation of

$$\chi_{\rm L}^{\rm YM} = \frac{1}{V}\Big\langle (n_+ - n_-)^2 \Big\rangle^{\rm YM}$$

is challenging for several reasons

- $L \sim 1$ fm and $a \sim 0.08$ fm $\Longrightarrow$ $\dim[D] \sim 2.5\ 10^5$: computing and diagonalizing the full matrix not feasible

- A standard minimization would require high precision to beat contamination from quasi-zero modes

- At large V the probability distribution has a width which increases linearly with V

$$P_Q = \frac{1}{\sqrt{2\pi V \chi_{\rm L}^{\rm YM}}} e^{-\frac{Q^2}{2V\chi_{\rm L}^{\rm YM}}} \{1 + O(V^{-1})\}$$

$\Longrightarrow$ computing $\chi_{\rm L}^{\rm YM}$ requires very high statistics

Algorithm for zero-mode counting

- In finite V null prob. for $n_+ \neq 0$ and $n_- \neq 0$

- Simultaneous minimization of Ritz functionals associated to

$$D^{\pm} = P_{\pm} D P_{\pm} \qquad P_{\pm} = \frac{1 \pm \gamma_5}{2}$$

to find the gap in one of the sectors

- Run again the minimization in the sector without gap and count zero modes

- No contamination from quasi-zero modes

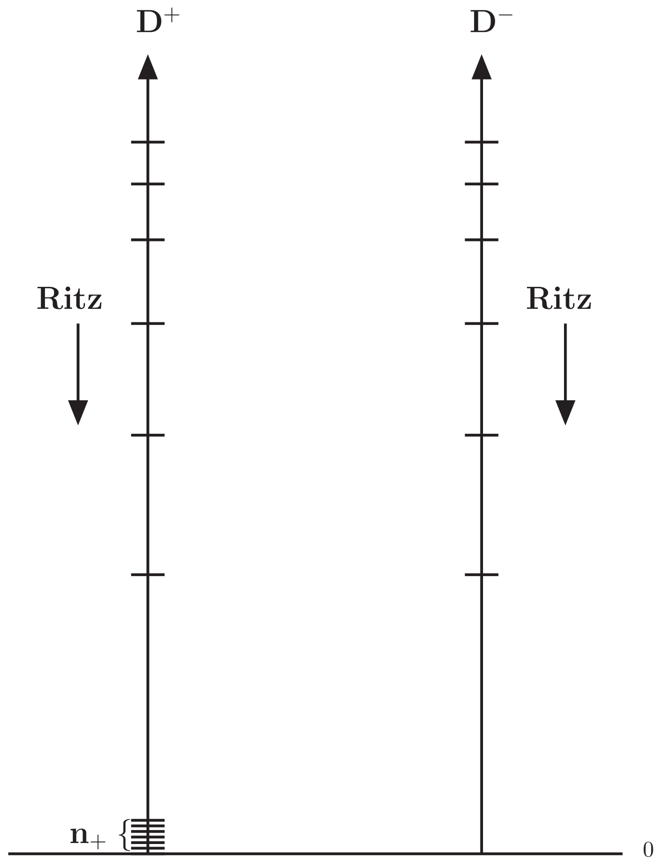

- With the GW definition a fit of the form

$$r_0^4 \chi^{\rm YM}(a,s) = r_0^4 \chi^{\rm YM} + c_1(s) \frac{a^2}{r_0^2}$$

gives

$$r_0^4 \chi^{\rm YM} = 0.059 \pm 0.003$$

- By setting the scale $F_{\rm K} = 109.6$ MeV

$$\chi^{\rm YM} = (0.185 \pm 0.005 \text{ GeV})^4$$

to be compared with

$$\frac{F^2}{2N_F}(M_\eta^2 + M_{\eta'}^2 - 2M_K^2) \underset{\rm exp}{\approx} (0.180 \text{ GeV})^4$$

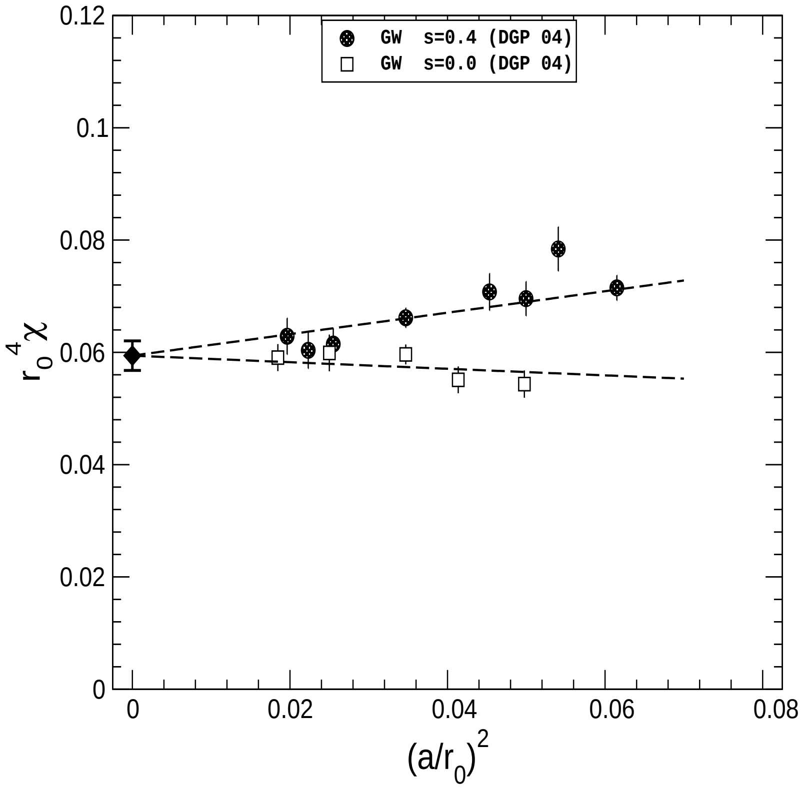

- The (leading) QCD anomalous contribution to $M_{\eta'}^2$ supports the Witten–Veneziano explanation for its large experimental value

Non-perturbative computation for $N_c = 3$ [Del Debbio et al. 04; Cè et al. 14]

- With the GW definition a fit of the form

$$r_0^4 \chi^{\rm YM}(a,s) = r_0^4 \chi^{\rm YM} + c_1(s)\,\frac{a^2}{r_0^2}$$

gives

$$r_0^4 \chi^{\rm YM} = 0.059 \pm 0.003$$

- By setting the scale $F_{\rm K} = 109.6$ MeV

$$\chi^{\rm YM} = (0.185 \pm 0.005\ {\rm GeV})^4$$

- With the Wilson flow definition

$$r_0^4 \chi^{\rm YM} = 0.054 \pm 0.002$$

which corresponds to

$$\chi^{\rm YM} = (0.181 \pm 0.004\ {\rm GeV})^4$$

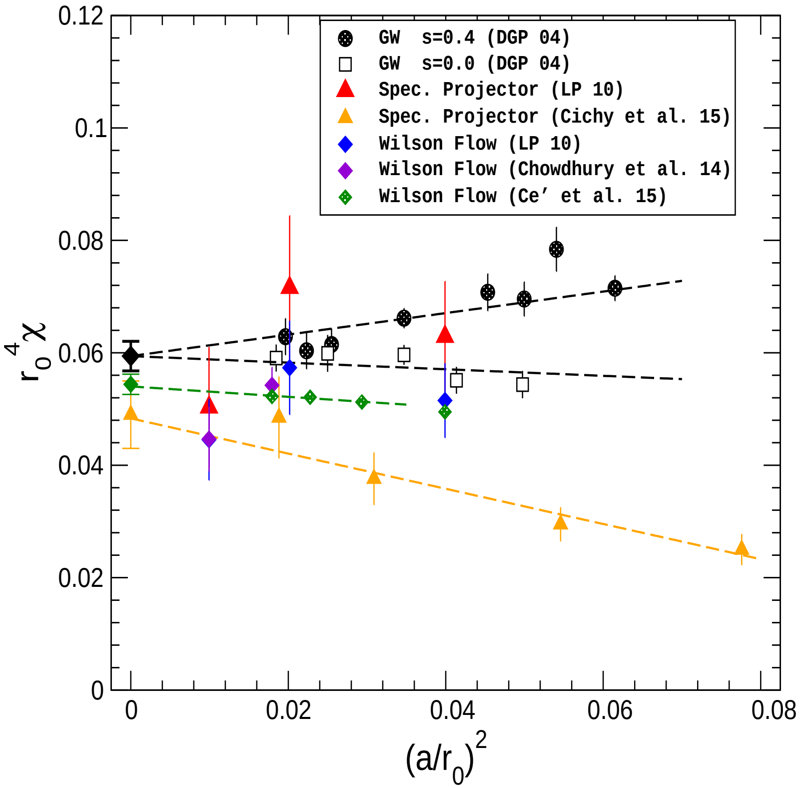

- From an unsolved problem to a universality test of lattice gauge theory!

- Vacuum energy and charge distribution are

$$e^{-F(\theta)} = \langle e^{i\theta Q}\rangle,\ P_Q = \int_{-\pi}^{\pi} \frac{d\theta}{2\pi} e^{-i\theta Q} e^{-F(\theta)}$$

Their behaviour is a distinctive feature of the configurations that dominate the path integr.

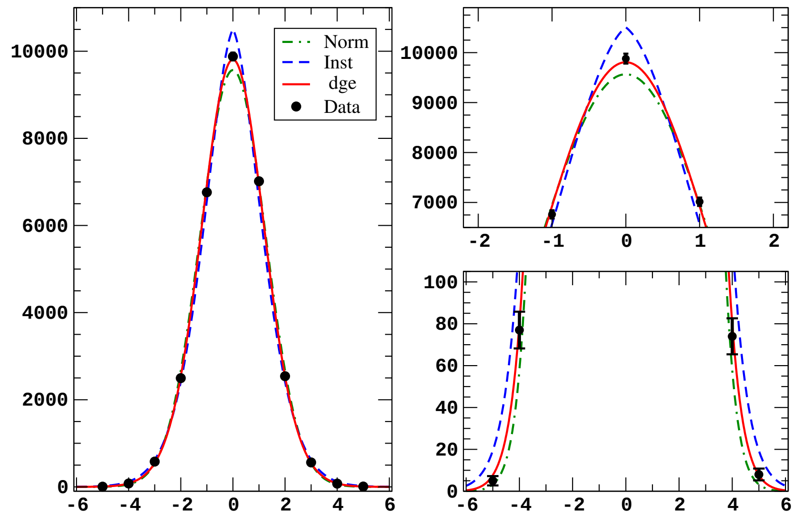

- Large N_c predicts ['t Hooft 74; Witten 79; Veneziano 79]

$$\frac{\langle Q^{2n}\rangle^{\rm con}}{\langle Q^2\rangle} \propto \frac{1}{N_c^{2n-2}}$$

- Various conjectures. For example, dilute-gas instanton model gives ['t Hooft 76; Callan et al. 76; ...]

$$F^{\rm Inst}(\theta) = -VA\{\cos(\theta) - 1\}$$

$$\frac{\langle Q^{2n}\rangle^{\rm con}}{\langle Q^2\rangle} = 1$$

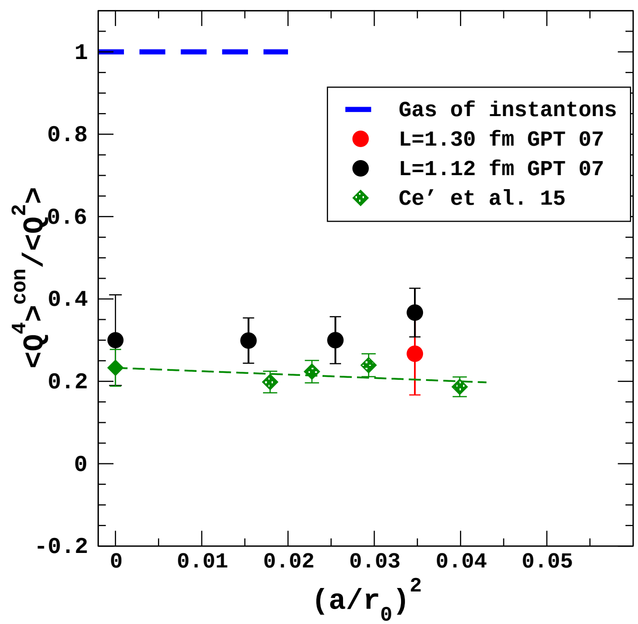

How the WV mechanism works ? [LG, Petrarca, Taglienti 07; Cè et al. 14]

- Vacuum energy and charge distribution are

$$e^{-F(\theta)} = \langle e^{i\theta Q}\rangle,\; P_Q = \int_{-\pi}^{\pi} \frac{d\theta}{2\pi} e^{-i\theta Q} e^{-F(\theta)}$$

Their behaviour is a distinctive feature of the configurations that dominate the path integr.

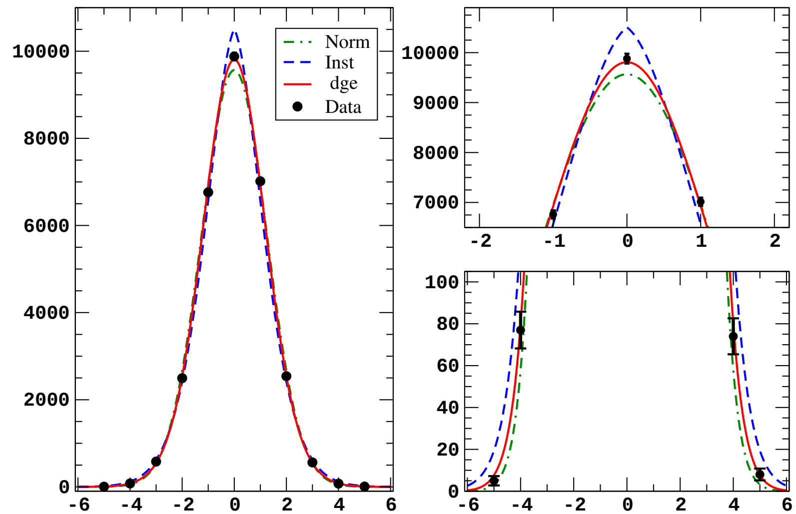

- Lattice computations give

$$\frac{\langle Q^4\rangle^{\rm con}}{\langle Q^2\rangle} = 0.30 \pm 0.11 \;\; \text{Ginsparg–Wilson}$$
$$= 0.23 \pm 0.05 \;\; \text{Wilson-Flow}$$

i.e. supports large N_c and disfavours a dilute gas of instantons

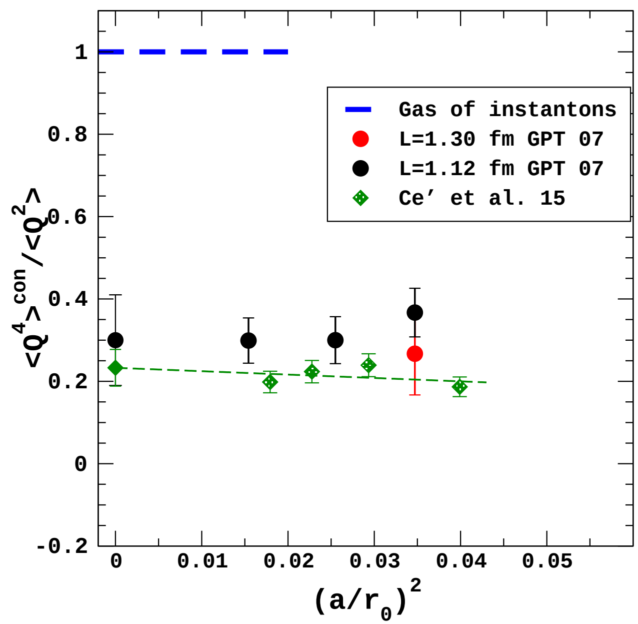

- The anomaly gives a mass to the η' thanks to the NP quantum fluctuations of Q

Broken symmetries and lattice gauge theory (IV): spontaneous symmetry breaking and the Banks–Casher relation

Leonardo Giusti

University of Milano-Bicocca

Light pseudoscalar meson spectrum

- Octet compatible with SSB pattern

$$\mathrm{SU}(3)_{\mathrm{L}} \times \mathrm{SU}(3)_{\mathrm{R}} \to \mathrm{SU}(3)_{\mathrm{L+R}}$$

and soft explicit symmetry breaking

$$m_u, m_d \ll m_s < \Lambda$$

- $m_u, m_d \ll m_s \Longrightarrow m_\pi \ll m_{\mathrm{K}}$

- A 9^{th} pseudoscalar with $m_{\eta'} \sim \mathcal{O}(\Lambda)$

I	I_3	S	Meson	Quark Content	Mass (GeV)
1	1	0	π^+	$u\bar{d}$	0.140
1	-1	0	π^-	$d\bar{u}$	0.140
1	0	0	π^0	$(d\bar{d} - u\bar{u})/\sqrt{2}$	0.135
$\frac{1}{2}$	$\frac{1}{2}$	+1	K^+	$u\bar{s}$	0.494
$\frac{1}{2}$	$-\frac{1}{2}$	+1	K^0	$d\bar{s}$	0.498
$\frac{1}{2}$	$-\frac{1}{2}$	-1	K^-	$s\bar{u}$	0.494
$\frac{1}{2}$	$\frac{1}{2}$	-1	$\overline{\mathrm{K}}^0$	$s\bar{d}$	0.498
0	0	0	η	$\cos\vartheta\eta_8 - \sin\vartheta\eta_0$	0.548
0	0	0	η'	$\sin\vartheta\eta_8 + \cos\vartheta\eta_0$	0.958

$$\begin{aligned} \eta_8 &= (d\bar{d} + u\bar{u} - 2s\bar{s})/\sqrt{6} \\ \eta_0 &= (d\bar{d} + u\bar{u} + s\bar{s})/\sqrt{3} \\ \vartheta &\sim -10^\circ \end{aligned}$$

QCD action and its (broken) symmetries

- QCD action for $N_F = 2$, $M^\dagger = M =$ diag(m, m)

$$S = S_G + \int d^4x \left\{ \bar\psi D \psi + \bar\psi_{\rm R} M^\dagger \psi_{\rm L} + \bar\psi_{\rm L} M \psi_{\rm R} \right\}, \qquad D = \gamma_\mu(\partial_\mu - i A_\mu)$$

- For $M = 0$ chiral symmetry

$$\psi_{\rm R,L} \to V_{\rm R,L}\psi_{\rm R,L} \quad \psi_{\rm R,L} = \left(\frac{1 \pm \gamma_5}{2}\right)\psi$$

Chiral anomaly: measure not invariant

SSB: vacuum not symmetric

$${\rm SU}(3)_c \times {\rm SU}(2)_{\rm L} \times {\rm SU}(2)_{\rm R} \times {\rm U}(1)_{\rm L} \times {\rm U}(1)_{\rm R} \times \mathcal{R}_{\rm scale}$$

↓ **(dim. transm., chiral anomaly)**

$${\rm SU}(3)_c \times {\rm SU}(2)_{\rm L} \times {\rm SU}(2)_{\rm R} \times {\rm U}(1)_{\rm B=L+R}$$

↓ **(Spont. Sym. Break.)**

$${\rm SU}(3)_c \times {\rm SU}(2)_{\rm L+R} \times {\rm U}(1)_{\rm B}$$

↓ (Confinement)

$${\rm SU}(2)_{\rm L+R} \times {\rm U}(1)_{\rm B}$$

- Breaking due to non-perturbative dynamics. Precise quantitative tests are being made on the lattice

Banks–Casher relation [Banks, Casher 80]

- The spectral density of D is

[Banks, Casher 80; Leutwyler, Smilga 92; Shuryak, Verbaarschot 93]

$$\rho(\lambda, m) = \frac{1}{V} \sum_k \langle \delta(\lambda - \lambda_k) \rangle$$

where $\langle \ldots \rangle$ indicates path-integral average

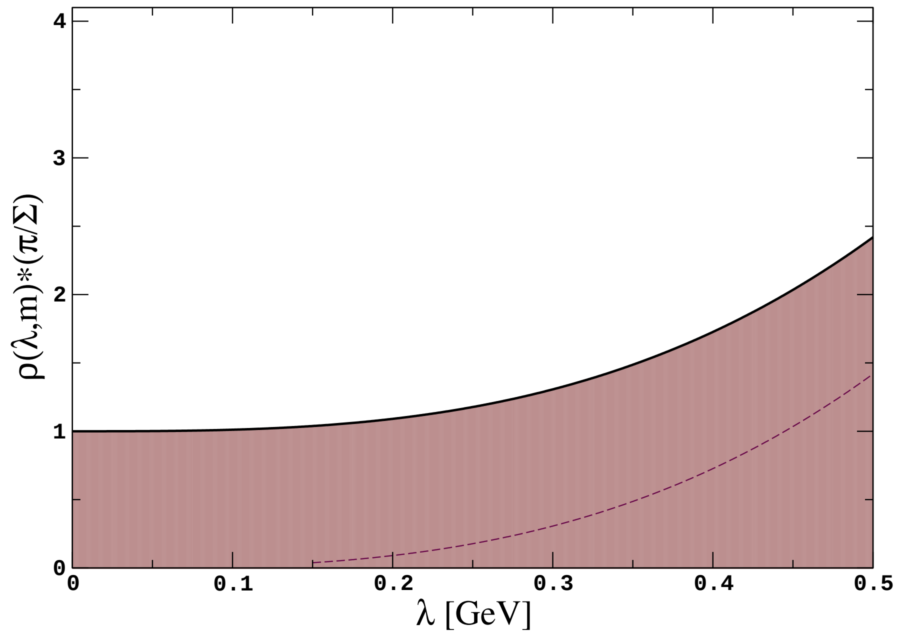

- The Banks–Casher relation

$$\lim_{\lambda \to 0} \lim_{m \to 0} \lim_{V \to \infty} \rho(\lambda, m) = \frac{\Sigma}{\pi}$$

can be read in both directions: a non-zero spectral density implies that the symmetry is broken with a non-vanishing Σ and vice versa.

To be compared, for instance, with the free case $\rho(\lambda) \propto |\lambda^3|$

Banks–Casher relation [Banks, Casher 80]

- The spectral density of D is

[Banks, Casher 80; Leutwyler, Smilga 92; Shuryak, Verbaarschot 93]

$$\rho(\lambda, m) = \frac{1}{V} \sum_k \langle \delta(\lambda - \lambda_k) \rangle$$

where $\langle \dots \rangle$ indicates path-integral average

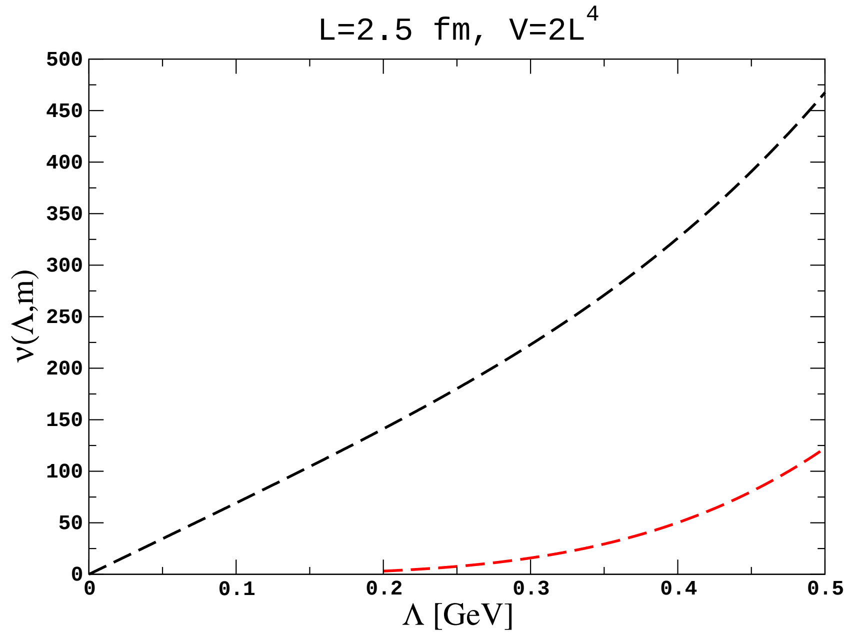

- The number of modes in a given energy interval

$$\nu(\Lambda, m) = V \int_{-\Lambda}^{\Lambda} d\lambda \; \rho(\lambda, m) \qquad \nu(\Lambda, m) = \frac{2}{\pi} \Lambda \Sigma V + \dots$$

grows linearly with Λ, and they condense near the origin with values $\propto 1/V$

In the free case $\nu(\Lambda, m) \propto V \Lambda^4$

Numerical computation for $N_{\rm f} = 2$ [Cichy et al. 13; Engel et al. 14]

- Twisted-mass QCD [Cichy et al. 13]:

  $*\ a = 0.054$–0.085 fm

  $*\ m = 16$–47 MeV

  $*\ M = 50$–120 MeV

  $*\ M = \sqrt{\Lambda^2 + m^2}$

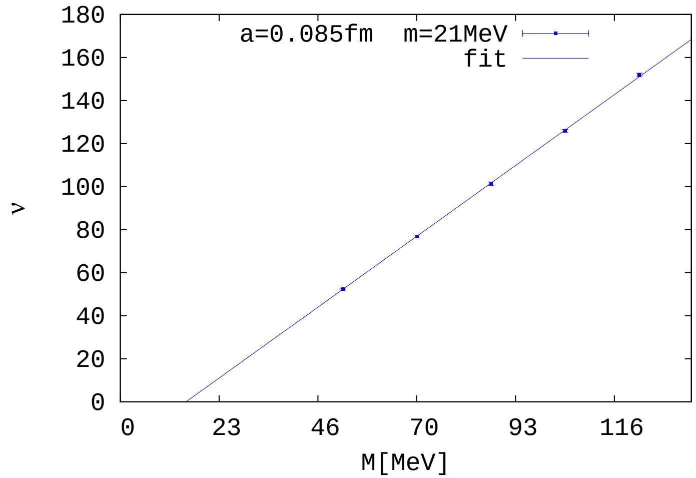

- $O(a)$–improved Wilson fermions [Engel et al. 14]:

  $*\ a = 0.048$–0.075 fm

  $*\ m = 6$–37 MeV

  $*\ \Lambda = 20$–500 MeV

  $*\ \nu = -9.0(13){+}2.07(7)\Lambda{+}0.0022(4)\Lambda^2$

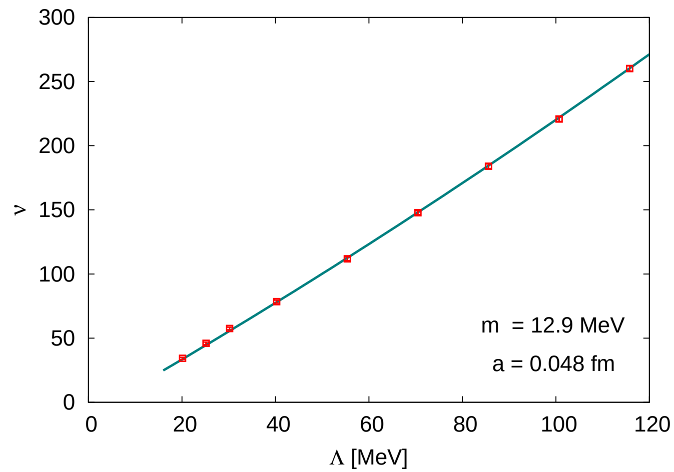

- The mode number is a nearly linear function in Λ up to approximatively 100 MeV. The modes do condense near the origin as predicted by the Banks–Casher mechanism

Numerical computation for $N_f = 2$ [Cichy et al. 13; Engel et al. 14]

- Twisted-mass QCD [Cichy et al. 13]:

  $* \ a = 0.054$–0.085 fm

  $* \ m = 16$–47 MeV

  $* \ M = 50$–120 MeV

  $* \ M = \sqrt{\Lambda^2 + m^2}$

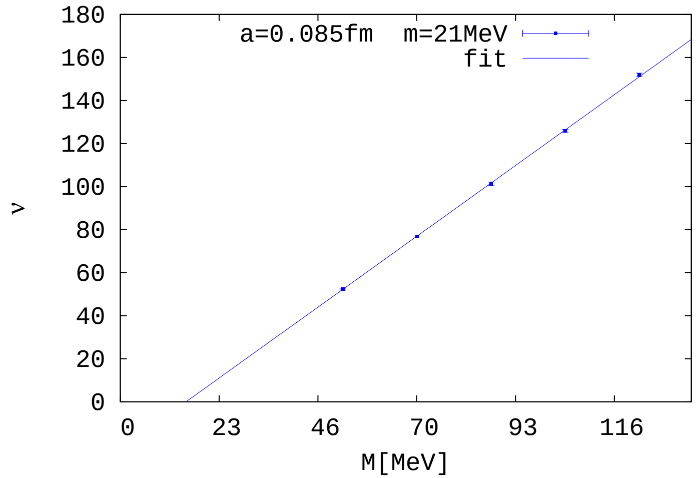

- $O(a)$–improved Wilson fermions [Engel et al. 14]:

  $* \ a = 0.048$–0.075 fm

  $* \ m = 6$–37 MeV

  $* \ \Lambda = 20$–500 MeV

  $* \ \nu = -9.0(13) + 2.07(7)\Lambda + 0.0022(4)\Lambda^2$

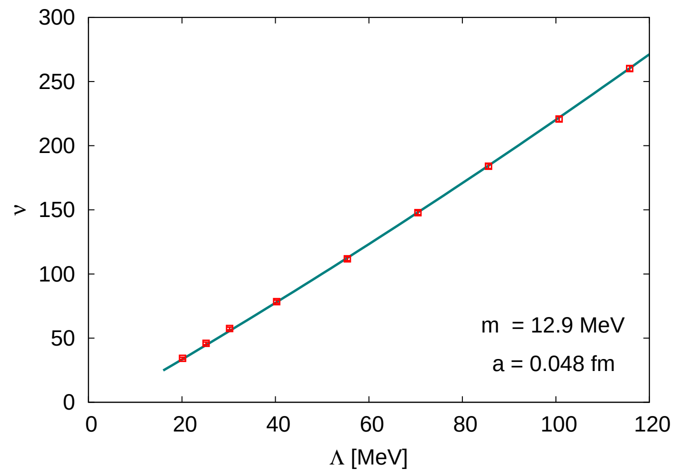

- At fixed lattice spacing and at the percent precision, however, data show statistically significant deviations from the linear behaviour of $O(10\%)$.

Continuum limit [Engel et al. 14]

- By defining

$$\widetilde{\rho}(\Lambda_1, \Lambda_2, m) = \frac{\pi}{2V} \frac{\nu(\Lambda_2) - \nu(\Lambda_1)}{\Lambda_2 - \Lambda_1}$$

the continuum limit is taken at fixed m, Λ_1 and Λ_2 [$\Lambda = (\Lambda_1 + \Lambda_2)/2$]

- Data are extrapolated linearly in a^2 as dictated by the Symanzik analysis

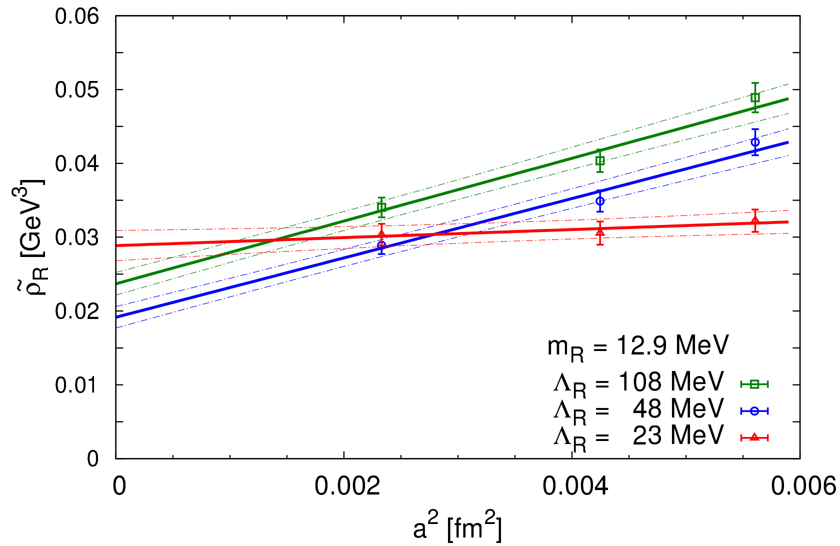

Continuum limit [Engel et al. 14]

- By defining

$$\widetilde{\rho}(\Lambda_1, \Lambda_2, m) = \frac{\pi}{2V} \frac{\nu(\Lambda_2) - \nu(\Lambda_1)}{\Lambda_2 - \Lambda_1}$$

the continuum limit is taken at fixed m, Λ_1 and Λ_2 [$\Lambda = (\Lambda_1 + \Lambda_2)/2$]

- Data are extrapolated linearly in a^2 as dictated by the Symanzik analysis

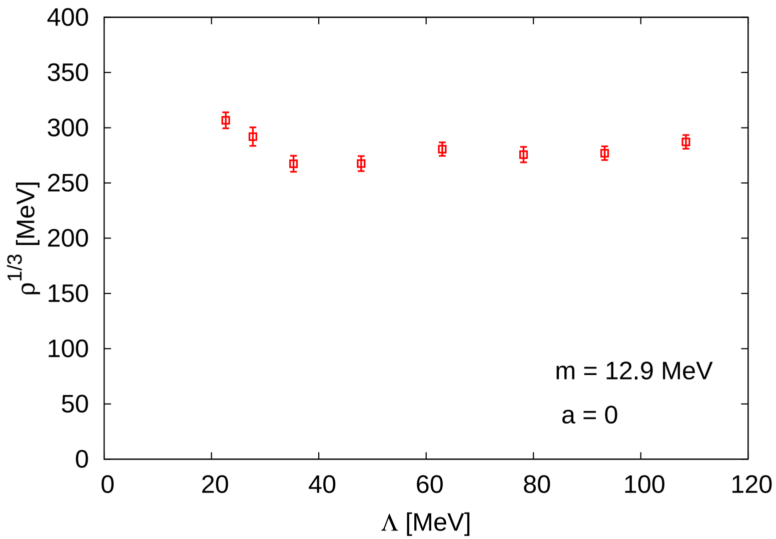

Continuum limit [Engel et al. 14]

- By defining

$$\widetilde{\rho}(\Lambda_1,\Lambda_2,m) = \frac{\pi}{2V}\,\frac{\nu(\Lambda_2)-\nu(\Lambda_1)}{\Lambda_2-\Lambda_1}$$

the continuum limit is taken at fixed m, Λ_1 and Λ_2 [$\Lambda = (\Lambda_1+\Lambda_2)/2$]

- Data are extrapolated linearly in a^2 as dictated by the Symanzik analysis

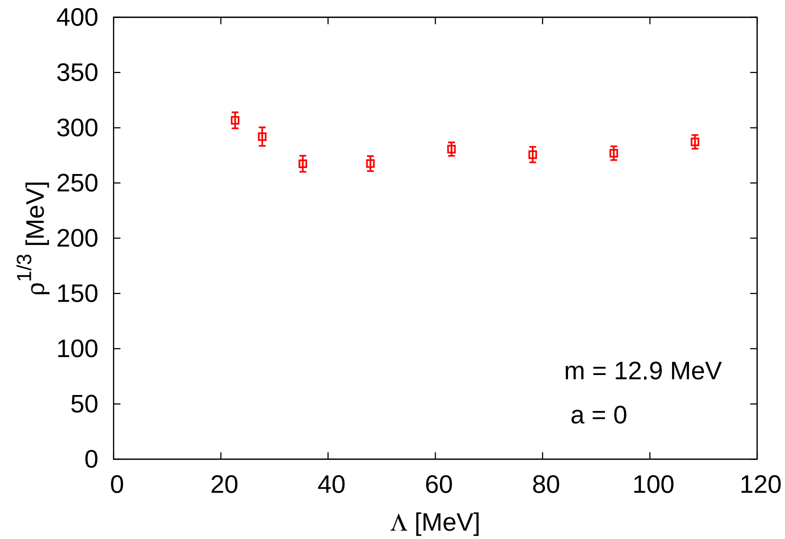

- It is noteworthy that no assumption on the presence of SSB was needed so far

- The results show that at small quark masses the spectral density is non-zero and (almost) constant in Λ near the origin

- Data are consistent with the expectations from the Banks–Casher mechanism in the presence of SSB. In this case NLO ChPT indeed predicts ($N_f = 2$)

$$\widetilde{\rho}^{\,\text{nlo}} = \Sigma\Big\{1+\frac{m\Sigma}{(4\pi)^2F^4}\Big[3\,\bar{l}_6+1-\ln(2)-3\ln\Big(\frac{\Sigma m}{F^2\bar{\mu}^2}\Big)+\tilde{g}_\nu\Big(\frac{\Lambda_1}{m},\frac{\Lambda_2}{m}\Big)\Big]\Big\}$$

Spectral density in ChPT [Osborn et al. 99; LG, Lüscher 09; Damgaard, Fukaya 09; Damgaard et al. 10; Necco, Shindler 11]

- When chiral symmetry is spontaneously broken, the spectral density can be computed in ChPT. At the NLO

$$\rho^{\rm nlo}(\lambda, m) = \frac{\Sigma}{\pi}\Big\{1 + \frac{m\Sigma}{(4\pi)^2 F^4}\Big[3\,\bar{l}_6 + 1 - \ln(2) - 3\ln\Big(\frac{\Sigma m}{F^2\bar{\mu}^2}\Big) + g_\nu\Big(\frac{\lambda}{m}\Big)\Big]\Big\}$$

where $g_\nu(x)$ is a parameter-free known function

- The NLO formula has properties which can be confronted against the NP results:

  ∗ at fixed λ no chiral logs are present when $m \to 0$

$$g_\nu(x) \xrightarrow{x\to\infty} -3\ln(x)$$

  ∗ in the chiral limit $\rho^{\rm nlo}(\lambda, m)$ becomes independent of λ
  This is an accident of the $N_{\rm f} = 2$ ChPT theory at NLO [Smilga, Stern 93]

  ∗ the λ dependence of $\rho^{\rm nlo}(\lambda, m)$ is a known function (up to overall constant).
  The spectral density is a slowly decreasing function of λ at fixed m

Chiral limit [Engel et al. 14]

- In the chiral limit NLO ChPT predicts $\widetilde{\rho}$ to be Λ-independent. By extrapolating to $m = 0$

$$[\widetilde{\rho}^{\,\overline{\rm MS}}]^{1/3} = [\Sigma^{\overline{\rm MS}}_{\rm BK}(2\,\text{GeV})]^{1/3} = 261(6)(8)\ \text{MeV}$$

where the spacing is fixed by introducing a quenched strange quark with $F_K = 109.6$ MeV

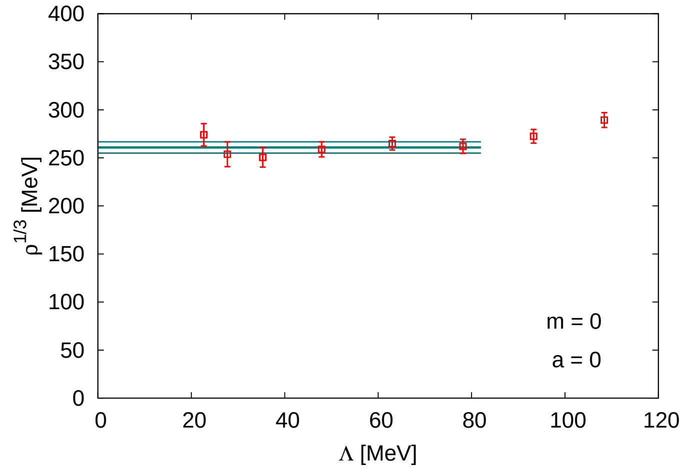

- In the chiral limit NLO ChPT predicts $\widetilde{\rho}$ to be Λ-independent. By extrapolating to $m = 0$

$$[\widetilde{\rho}^{\,\overline{\rm MS}}]^{1/3} = [\Sigma^{\overline{\rm MS}}_{\rm BK}(2\,\text{GeV})]^{1/3} = 261(6)(8)\,\text{MeV}$$

where the spacing is fixed by introducing a quenched strange quark with $F_K = 109.6$ MeV

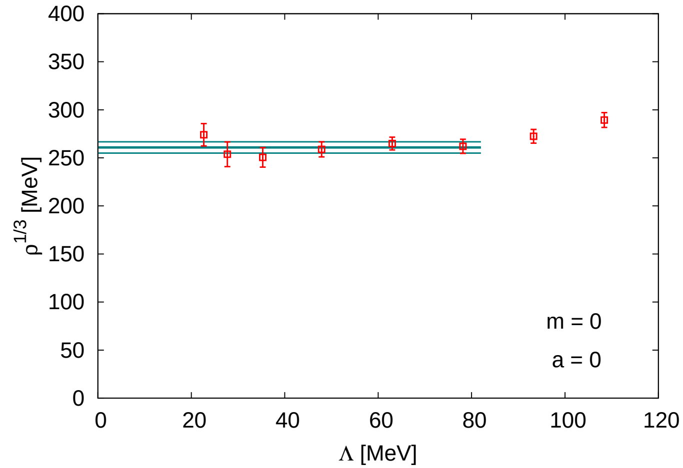

- The distinctive signature of SSB is the agreement between $\widetilde{\rho}$ and the slope of $M_\pi^2 F_\pi^2/2$ with respect to m in the chiral limit

- On the same set of configurations by fitting the data with NLO (W)ChPT for $M_\pi < 400$ MeV

$$[\Sigma^{\overline{\rm MS}}_{\rm GMOR}(2\,\text{GeV})]^{1/3} = 263(3)(4)\,\text{MeV}$$

to be compared with the previous result

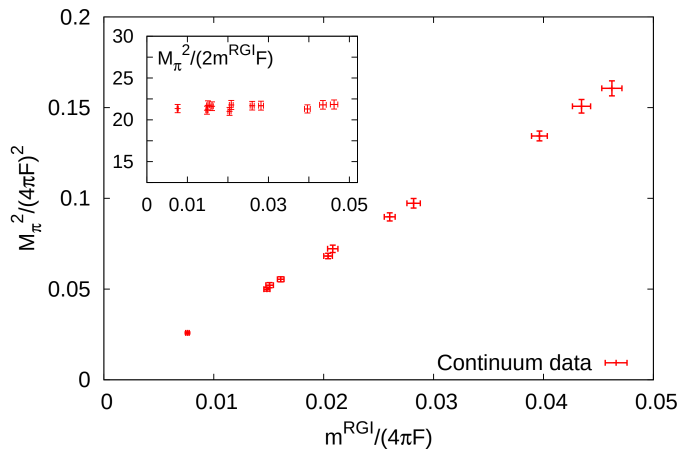

Chiral limit [Engel et al. 14]

- In the chiral limit NLO ChPT predicts $\widetilde{\rho}$ to be Λ-independent. By extrapolating to $m = 0$

$$[\widetilde{\rho}^{\,\overline{\rm MS}}]^{1/3} = [\Sigma_{\rm BK}^{\overline{\rm MS}}(2\,\text{GeV})]^{1/3} = 261(6)(8)\,\text{MeV}$$

where the spacing is fixed by introducing a quenched strange quark with $F_K = 109.6$ MeV

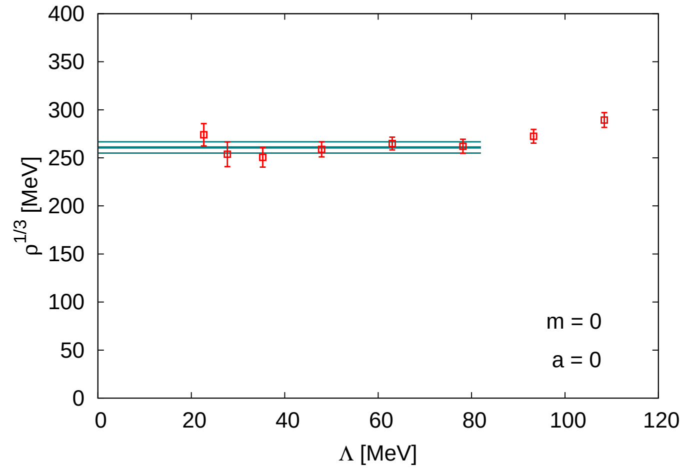

- The distinctive signature of SSB is the agreement between $\widetilde{\rho}$ and the slope of $M_\pi^2 F_\pi^2/2$ with respect to m in the chiral limit

- On the same set of configurations by fitting the data with NLO (W)ChPT for $M_\pi < 400$ MeV

$$[\Sigma_{\rm GMOR}^{\overline{\rm MS}}(2\,\text{GeV})]^{1/3} = 263(3)(4)\,\text{MeV}$$

to be compared with the previous result

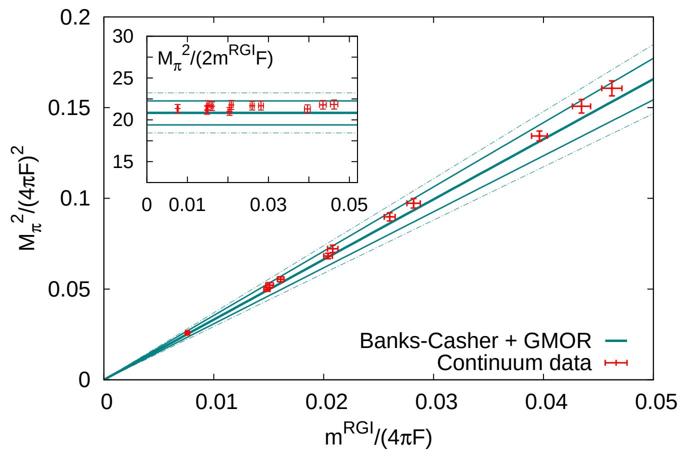

Gell-Mann–Oakes–Renner relation

- The spectral density of the Dirac operator in the continuum is $\neq 0$ at the origin for $m = 0$

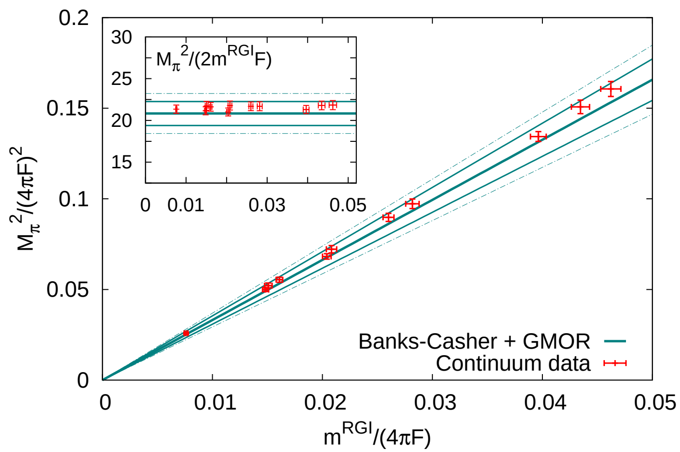

- The low-modes of the Dirac operator do condense following Banks–Casher mechanism

- The rate of condensation agrees with the GMOR relation, and it explains the bulk of the pion mass up to $M_\pi \leq 500$ MeV

- The dimensionless ratios

$$[\Sigma^{\rm RGI}]^{1/3}/F = 2.77(2)(4)\ , \quad \Lambda^{\overline{\rm MS}}/F = 3.6(2)$$

are "geometrical" properties of the theory. They belong to the category of unambiguous quantities in the two flavour theory that should be used for quoting and comparing results rather than those expressed in physical units

- They can be directly compared with your preferred approximation/model

Summary

- An impressive global (lattice) community effort to reach a precise quantitative understanding of the behaviour of QCD in the chiral regime from first principles

- The spectral density of the Dirac operator in the continuum and chiral limits is $\neq 0$ at the origin. The rate of condensation explains the bulk of the pion mass up to $M_\pi \leq 500$ MeV

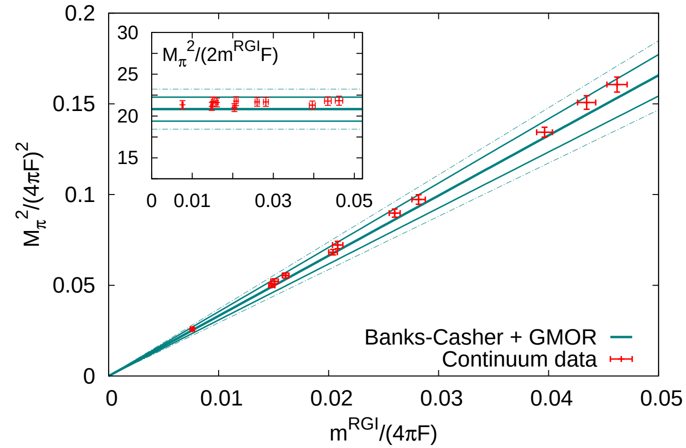

- All numerical results for $\chi^{\rm YM}$ are consistent with the conceptual progress made over the last decade. A percent precision reached. Universality is at work if χ is (properly) defined on the lattice!

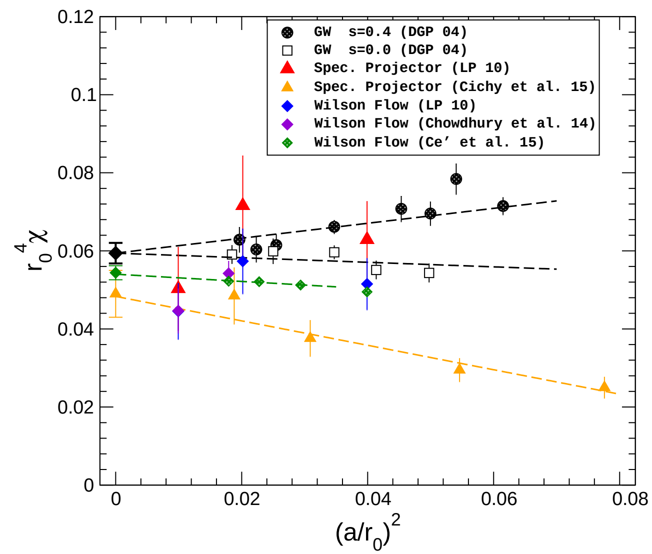

- The (leading) QCD anomalous contribution to $M_{\eta'}^2$ supports the Witten–Veneziano explanation for its large experimental value